JHEP

Published by IOP Publishing for SISSA

Received: *September 22, 2009*
Accepted: *October 30, 2009*
Published: *November 16, 2009*

Minimal Z' models: present bounds and early LHC reach

Ennio Salvioni,[a] **Giovanni Villadoro**[b] **and Fabio Zwirner**[c]

[a] *Dipartimento di Fisica, Università di Padova and INFN, Sezione di Padova, Via Marzolo 8, I-35131 Padova, Italy*
[b] *Theory Group, Physics Department, CERN, CH–1211 Geneva 23, Switzerland*
[c] *Dipartimento di Fisica, Università di Padova and INFN, Sezione di Padova, Via Marzolo 8, I-35131 Padova, Italy*

E-mail: ennio.salvioni@pd.infn.it, giovanni.villadoro@cern.ch, fabio.zwirner@pd.infn.it

Abstract: We consider 'minimal' Z' models, whose phenomenology is controlled by only three parameters beyond the Standard Model ones: the Z' mass and two effective coupling constants. They encompass many popular models motivated by grand unification, as well as many arising in other theoretical contexts. This parameterization takes also into account both mass and kinetic mixing effects, which we show to be sizable in some cases. After discussing the interplay between the bounds from electroweak precision tests and recent direct searches at the Tevatron, we extend our analysis to estimate the early LHC discovery potential. We consider a center-of-mass energy from 7 towards 10 TeV and an integrated luminosity from 50 to several hundred pb^{-1}, taking all existing bounds into account. We find that the LHC will start exploring virgin land in parameter space for $M_{Z'}$ around 700 GeV, with lower masses still excluded by the Tevatron and higher masses still excluded by electroweak precision tests. Increasing the energy up to 10 TeV, the LHC will start probing a wider range of Z' masses and couplings, although several hundred pb^{-1} will be needed to explore the regions of couplings favored by grand unification and to overcome the Tevatron bounds in the mass region around 250 GeV.

Keywords: Beyond Standard Model, Hadronic Colliders, GUT

ArXiv ePrint: 0909.1320

doi:10.1088/1126-6708/2009/11/068

JHEP11(2009)068

Contents

1 Introduction and summary **1**

2 Theory **4**
- 2.1 Parameterization 4
- 2.2 Constraints from grand unification 6

3 Present bounds **8**
- 3.1 Electroweak precision tests 8
- 3.2 Tevatron direct searches 10
- 3.3 Comparison among different bounds 11

4 Early LHC prospects **15**

JHEP11(2009)068

1 Introduction and summary

Among the extensions of the Standard Model (SM) at the TeV scale, those with an additional U(1) factor in the gauge group, associated with a heavy neutral gauge boson Z', have often been considered in direct and indirect searches for new physics, and in the studies of possible early discoveries at the LHC (for recent reviews and references, see e.g. [1]). While not prescribed by compelling theoretical or phenomenological arguments, these extensions naturally arise from Grand Unified Theories (GUTs) based on groups of rank larger than four and from higher-dimensional constructions such as string compactifications. Z' bosons also appear in little Higgs models, composite Higgs models, technicolor models and other more or less plausible scenarios for physics at the Fermi scale.

Many varieties of Z' models have been considered over the years [1]. In the following, we will concentrate on a class of *minimal* models, previously discussed in [2], that stands out for its simplicity and for the small number of additional free parameters with respect to the SM ones. Nevertheless, this class is sufficiently rich and motivated to emerge as a natural benchmark for comparing direct and indirect signals in different experimental contexts, in particular for organizing experimental searches at present hadron colliders such as the Tevatron and the LHC.

By *minimal* Z' models we mean the most economical U(1) extensions of the SM that do not spoil renormalizability. Making reference to the SM particle content, our minimality requirements can be summarized as follows: no exotic vectors, apart from a single Z' associated with a U(1) factor in the gauge group, commuting with $G_{\rm SM} = {\rm SU}(3)_C \times {\rm SU}(2)_L \times {\rm U}(1)_Y$; no exotic fermions, apart from one right-handed neutrino, singlet under $G_{\rm SM}$, for each of the three SM families, and family-independent but generically non-vanishing U(1) charges; no exotic scalars beyond the SM Higgs field, meaning that

the extra U(1) factor in G is either broken explicitly (which is still compatible with renormalizability), or that the possible non-SM scalars from the extended Higgs sector can be neglected in the first Z' 'discovery studies', because they are sufficiently heavy and/or sufficiently decoupled from the SM fields, including the SM Higgs.

The introduction of right-handed neutrinos makes it possible to generate a realistic pattern of neutrino masses (Dirac and Majorana) via renormalizable interactions. Similarly, it is possible to cancel all gauge and gravitational anomalies without introducing exotic fermions (as is instead required in some E_6 models) and/or non-renormalizable anomaly-canceling terms (as in some string-inspired models), as long as the generator of the additional U(1) factor is a linear combination of the weak hypercharge Y and of baryon-minus-lepton number, $B-L$. Also, our minimal class of models interpolates continuously among several discrete examples already considered in the literature: the 'pure $B-L$' model, the 'χ' model arising from SO(10) unification, left-right symmetric models, etc. Minimal Z' models can be extended to include supersymmetry, but the price to pay is the introduction of many free parameters associated with the supersymmetric particle spectrum: for this reason we will restrict ourselves to the minimal case, commenting on the possible effects of light supersymmetric particles when relevant.

As we shall see, the simplicity of the parameterization allows us to perform a relatively model-independent study, which does not focus on a fixed type or size of Z' couplings and automatically takes into account mixing effects, both in the mass terms and in the kinetic terms, such as those generated in the evolution under the renormalization group equations (RGE). We find that the latter effects are indeed quite important, even for relatively weakly coupled Z'.

With the parameterization above, we perform an updated analysis of the present indirect bounds coming from electroweak precision tests (EWPT), including LEP2 and other experiments at low energy, and of the recent limits from direct searches at the Tevatron, taking into account the effects of mixing when necessary. Contrary to the common lore, we find that models with no $Z-Z'$ mixing, such as pure $B-L$ models, are as constrained as other models; actually, they are even more constrained than those with a partial cancellation of some suitable effective charge, such as the χ model.

Our goal is to apply our parameterization to study the impact of the present bounds on the discovery reach of the LHC, especially in the early phase when energy and luminosity will be limited. We find that the first virgin land in parameter space that will become accessible to the LHC will correspond to relatively weakly coupled and light Z', with masses of 600-800 GeV, while Z' bosons of the kind favored by GUTs, which are forced to be heavier by the present bounds, will require some more energy and luminosity to become accessible. We will show that indeed the unexplored region of parameter space — masses and types of Z' couplings — that will become accessible at each energy and luminosity, especially during the first LHC runs, depends non-trivially on the present bounds. This makes the use of a model-independent parameterization, such as the one suggested in this work, a valuable tool to systematically organize the Z' searches.

Our paper is organized as follows. In section 2, we elaborate on some results of [2] and illustrate how, in our minimal class of models, the main Z' properties and its couplings

JHEP11(2009)068

to the SM states can be very simply described in terms of just three new parameters beyond the SM ones: the Z' mass, $M_{Z'}$, and two effective coupling constants, g_Y and $g_{\rm BL}$, associated to the Y and $B-L$ currents, respectively.[1] Such parameterization automatically takes into account all mixing effects in the gauge boson sector, both in the kinetic terms and in the mass matrix. In contrast with GUT-inspired parameterizations, often used for interpreting experimental searches, our parameterization also allows for relatively weak Z' couplings to the SM fermions: such a situation is disfavored by conventional GUTs but could arise, for example, in anisotropic string compactifications. To give a flavor of the generic GUT constraints, we solve the one-loop RGE for the above coupling constants, both in the non-supersymmetric and in the supersymmetric case, showing that the large hierarchy between the GUT scale and the weak scale generically induces sizable kinetic mixing effects from the running, even for moderate values of the coupling constants. We then identify both the region of parameter space generically favored by GUTs and some points in parameter space corresponding to 'true' GUT-models, comparing them with some conventional benchmark points often used in the literature. In section 3, we review the present bounds on the Z' parameter space. We start by discussing the impact of EWPT, including those from LEP2 and atomic parity violation (APV), applying the methods and the results of [3]. In addition, we discuss the impact of some later reanalysis of APV [4], to conclude that the electroweak fit of [3] still gives the most stringent constraints. Then we discuss the bounds coming from direct searches at the Tevatron, including the most recent data from CDF [5, 6] and D0 [7]. We confirm that, as for the models considered in previous studies [8–11], EWPT are more stringent than Tevatron direct searches for relatively heavy and relatively strongly coupled Z', such as the ones predicted by GUTs. On the other hand, Tevatron searches are more stringent than EWPT for relatively light and relatively weakly coupled Z', disfavored by GUTs but potentially permitted by other models. As a representative example, we comment on the possible excess in the CDF e^+e^- sample [5] at an invariant mass near 240 GeV: the size of the effect would correspond to a rather weakly coupled Z', disfavored by GUTs but still allowed by EWPT. We conclude in section 4 with a study of the prospects for the first LHC run(s). The main question we address is what energy and luminosity are needed to explore virgin land in parameter space, and how much of such accessible new territory is compatible with conventional GUTs. We show that, with the foreseen schedule for the first year [12] of the LHC (first 50-100 pb^{-1} at $\sqrt{s} = 7$ TeV, then up to 200$\div$300 pb^{-1} at $\sqrt{s} \leq 10$ TeV), the first region in parameter space to be explored will correspond to moderately light and weakly coupled Z', weighing around 600-800 GeV, and with a small window of allowed couplings. To open up considerably the region of parameter space accessible for discoveries, in particular the one relevant to GUT models, at least $O(1)$ fb^{-1} of integrated luminosity should be collected. In summary, in the very first phase of the LHC the interplay among center-of-mass energy, integrated luminosity and previous direct and indirect bounds will be quite subtle, and it will be important to focus the analysis onto the most promising regions of parameter space, possibly combining different channels and experiments from the very beginning.

[1] The reader should not confuse g_Y with the SM U(1)$_Y$ gauge coupling constant, which we denote by g', with g denoting the SU(2)$_L$ gauge coupling constant.

JHEP11(2009)068

2 Theory

2.1 Parameterization

As discussed in the Introduction, we will consider extensions of the SM where $G_{\rm SM}$ is extended by a single additional non-anomalous family-independent U(1) factor, in the presence of three full SM fermion families, including right-handed neutrinos. As for the Higgs sector of the theory, we will assume the existence of the SM Higgs field but avoid as much as possible any specific assumption on the symmetry breaking mechanism for the additional U(1).

As previously discussed in [2], it is not restrictive to parameterize masses, kinetic mixing [13] and interactions with fermions for our extended neutral electroweak sector by means of the following effective Lagrangian:

$$\mathcal{L} = -\frac{1}{4}\, h_{AB}\, F^A_{\mu\nu}\, F^{B\,\mu\nu} + \frac{1}{2}\, M^2_{AB}\, A^{A\mu}\, A^B_\mu + A^A_\mu\, J^\mu_A + \dots\,, \tag{2.1}$$

where $A, B = T_{3L}, Y, B-L$. It is also well known that, by appropriate field redefinitions, we can go to a field basis where kinetic terms are canonical and masses are diagonal:

$$\mathcal{L} = -\frac{1}{4}\, F^i_{\mu\nu}\, F^{i\,\mu\nu} + \frac{1}{2}\, M^2_i A^{i\mu}\, A^i_\mu + A^i_\mu\, J^\mu_i + \dots\,, \tag{2.2}$$

where $i = \gamma, Z, Z'$. In the above equation, M_γ, M_Z and $M_{Z'}$ are the mass eigenvalues. The currents J^μ_i $(i = \gamma, Z, Z')$ are those coupled to the gauge boson mass eigenstates. For example,

$$J^\mu_\gamma = e \sum_f Q(f)\, \overline{f}\gamma^\mu f \tag{2.3}$$

is the electromagnetic current, where f runs over the different chiral projections of the SM fermions, $Q(f) = T_{3L}(f) + Y(f)$ is their electric charge, and the contributions from the scalar sector have been omitted. Similarly, we can write

$$J^\mu_Z = \cos\theta'\, J^\mu_{Z^0} - \sin\theta'\, J^\mu_{Z'^0}\,, \qquad J^\mu_{Z'} = \sin\theta'\, J^\mu_{Z^0} + \cos\theta'\, J^\mu_{Z'^0}\,, \tag{2.4}$$

where

$$J^\mu_{Z^0} = g_Z \sum_f \left[T_{3L}(f) - \sin^2\theta_W\, Q(f)\right]\, \overline{f}\gamma^\mu f\,, \qquad \left(g_Z = \sqrt{g^2 + g'^2}\right)\,, \tag{2.5}$$

is the SM expression for the current coupled to the SM Z^0 (we recall that, in the presence of mixing, Z^0 does not coincide with the mass eigenstate Z), and

$$\begin{aligned} J^\mu_{Z'^0} &= \sum_f \left[g_Y\, Y(f) + g_{\rm BL}\, (B-L)(f)\right]\, \overline{f}\gamma^\mu f \\ &= \sum_f g_Z\, Q_{Z'}(f)\, \overline{f}\gamma^\mu f\,. \end{aligned} \tag{2.6}$$

Again, possible contributions to the currents from the scalar sector have been omitted. We collected in table 1 the charges of the SM fermions needed for evaluating the currents of

JHEP11(2009)068

	(u,d)	u^c	d^c	(ν,e)	ν^c	e^c
T_{3L}	$\left(+\frac{1}{2},-\frac{1}{2}\right)$	0	0	$\left(+\frac{1}{2},-\frac{1}{2}\right)$	0	0
Y	$+\frac{1}{6}$	$-\frac{2}{3}$	$+\frac{1}{3}$	$-\frac{1}{2}$	0	$+1$
$B-L$	$+\frac{1}{3}$	$-\frac{1}{3}$	$-\frac{1}{3}$	-1	$+1$	$+1$
$Q_{Z'}$	$\frac{1}{6}\widetilde{g}_Y+\frac{1}{3}\widetilde{g}_{\rm BL}$	$-\frac{2}{3}\widetilde{g}_Y-\frac{1}{3}\widetilde{g}_{\rm BL}$	$\frac{1}{3}\widetilde{g}_Y-\frac{1}{3}\widetilde{g}_{\rm BL}$	$-\frac{1}{2}\widetilde{g}_Y-\widetilde{g}_{\rm BL}$	$\widetilde{g}_{\rm BL}$	$\widetilde{g}_Y+\widetilde{g}_{\rm BL}$

Table 1. The charges of left-handed fermions controlling the electroweak neutral currents.

eqs. (2.5) and (2.6). For definiteness, we chose a purely left-handed basis for the fermion fields, so that, omitting family indices, $f = u, d, u^c, d^c, \nu, e, \nu^c, e^c$. In expressing the charges $Q_{Z'}$, we found it convenient to make reference to the ratios

$$\widetilde{g}_Y = \frac{g_Y}{g_Z}\,, \qquad \widetilde{g}_{\rm BL} = \frac{g_{\rm BL}}{g_Z}\,. \tag{2.7}$$

The parameterization above automatically contains and extends specific models often considered in the literature, such as Z_{B-L}, Z_χ, and Z_{3R} models, whose couplings simply read, in our notation:

	Z_{B-L}	Z_χ	Z_{3R}
g_Y	0	$-\frac{2}{\sqrt{10}}g_{Z'}$	$-\,g_{Z'}$
g_{B-L}	$\sqrt{\frac{3}{8}}g_{Z'}$	$\frac{5}{2\sqrt{10}}g_{Z'}$	$\frac{1}{2}g_{Z'}$

, (2.8)

where $g_{Z'}$ is usually fixed to a 'GUT-inspired' value $g_{Z'} = \sqrt{5/3}\,g'$.

Since the SM Higgs doublet H has[2] vanishing $B-L$, and, as discussed in [2], it is not restrictive to take the Higgs fields that break $B-L$ (if any) to have vanishing Y, we can express the $Z-Z'$ mixing angle θ' in terms of g_Y and $M_{Z'}$,

$$\tan\theta' = -\widetilde{g}_Y\,\frac{M_{Z^0}^2}{M_{Z'}^2 - M_{Z^0}^2}\,, \tag{2.9}$$

where

$$M_{Z^0}^2 = \frac{g_Z^2\,v^2}{4} \tag{2.10}$$

is the SM expression for the Z^0 mass. The same remains true if we assume that there is an explicit (or Stückelberg-like) diagonal mass term for the $Z^{0\prime}$, without introducing an additional complex Higgs field for breaking $B-L$.

Notice that the mixing angle is completely determined by the mass and the couplings of the Z'. In particular, it is always non-vanishing whenever $\widetilde{g}_Y \neq 0$ (i.e. for models different from pure $B-L$), because in these cases gauge invariance of the Yukawa terms forces the SM Higgs to be charged under the extra U(1), thus producing a $Z-Z'$ mixing.

We can then study the Z' phenomenology in terms of three unknown parameters: the Z' mass $M_{Z'}$ and the two coupling constants $(g_Y, g_{\rm BL})$ or, equivalently, $(\widetilde{g}_Y, \widetilde{g}_{\rm BL})$.

[2]This property is shared by the MSSM Higgs doublets H_1 and H_2.

JHEP11(2009)068

We will not consider possible additional parameters of the enlarged Higgs sector and the right-handed neutrino masses, because, as will be discussed later, these parameters will play a relatively minor rôle in the following. To be definite, we will assume that there are three mostly left-handed neutrinos lighter than $O(1)\,\text{eV}$ and three mostly right-handed neutrinos heavier than $M_{Z'}/2$, as in the see-saw mechanism, and that the physical components of the Higgs fields whose VEVs break $B-L$ (if any) have negligible mixing with the SM Higgs and masses larger than $M_{Z'}$.

2.2 Constraints from grand unification

One of the possible motivations for considering Z' models are GUTs, with or without supersymmetry. Through appropriate boundary conditions at the unification scale M_U and RGE on the running gauge coupling constants, GUTs can constrain the range of some low-energy Z' parameters, such as the coupling constants g_Y and g_{BL}. The most stringent constraints can be obtained within specific models, where the full particle spectrum is specified and threshold and higher-loop corrections can be computed. Here, instead, we would like to remain as model-independent as possible within the general class of minimal Z' models. To this end, we will identify a GUT-favored region in the $(\widetilde{g}_Y, \widetilde{g}_{\text{BL}})$ plane[3] according to the following procedure.

First, we recall that the gauge coupling constants g', g_Y, g_{BL} are related to the 2×2 submatrix h_{AB} with $A,B=\{Y,B-L\}$ appearing in eq. (2.1), via

$$h_{AB}=\begin{pmatrix} \dfrac{1}{g'^2} & -\dfrac{g_Y}{g_{\text{BL}}}\dfrac{1}{g'^2} \\ -\dfrac{g_Y}{g_{\text{BL}}}\dfrac{1}{g'^2} & \dfrac{1}{g_{\text{BL}}^2}+\dfrac{g_Y^2}{g_{\text{BL}}^2}\dfrac{1}{g'^2} \end{pmatrix}. \tag{2.11}$$

The matrix h_{AB} obeys simple one-loop RGEs, which can be solved analytically:

$$h_{AB}(M_U)=h_{AB}(M_Z)-\frac{b_{AB}}{(4\pi)^2}\log\left(\frac{M_U}{M_Z}\right)^2, \tag{2.12}$$

where

$$b_{AB}=\frac{2}{3}\sum_f Q_f^A Q_f^B+\frac{1}{3}\sum_s Q_s^A Q_s^B\,, \tag{2.13}$$

and s are the complex scalars in the theory. We collect some representative values of the b_{AB} coefficients in table 2, always including the contribution of the three fermion families of table 1, and adding:

(i) only the SM Higgs field, $H\sim(1,2,+1/2,0)$;

(ii) the SM Higgs field H plus a complex SM-singlet scalar $\phi\sim(1,1,0,+2)$;

[3] All the results are insensitive to the transformation $(\widetilde{g}_Y,\widetilde{g}_{\text{BL}})\to(-\widetilde{g}_Y,-\widetilde{g}_{\text{BL}})$, without lack of generality we will thus consider only the upper half plane $\widetilde{g}_{\text{BL}}>0$.

JHEP11(2009)068

	(i)	(ii)	(iii)	(iv)
b_{YY}	41/6	41/6	11	11
$b_{Y(B-L)}$	16/3	16/3	8	8
$b_{(B-L)(B-L)}$	32/3	12	16	24

Table 2. The b_{AB} coefficients for the four representative cases defined in the text.

(iii) spin-0 superpartners for all the quarks and leptons in table 1, spin-1/2 superpartners for all the gauge bosons, and two Higgs chiral superfields $H_1 \sim (1, 2, -1/2, 0)$ and $H_2 \sim (1, 2, +1/2, 0)$, as in the MSSM;

(iv) all the fields of the previous case, plus two extra chiral superfields $\phi_1 \sim (1, 1, 0, -2)$ and $\phi_2 \sim (1, 1, 0, +2)$.

The quantum numbers in brackets denote, in a self-explanatory notation, the representations of $\mathrm{SU}(3)_C$, $\mathrm{SU}(2)_L$, $\mathrm{U}(1)_Y$ and $\mathrm{U}(1)_{\mathrm{BL}}$.

For choosing the boundary conditions at the GUT scale M_U, we normalize all U(1) charges as in SO(10), and we take $M_U = 10^{16}\,\mathrm{GeV}$ as a reference value. In typical GUTs, M_U can vary within approximately two decades around such reference value, but the difference in our estimate of the GUT-favored region is of the order of other threshold effects that we reabsorbed in the wide ranges we assume below for other parameters. Then, we compute the boundary value $g'(M_U)$ using the phenomenological input $g'(M_Z) = e(M_Z)/\cos\theta_W(M_Z)$, with $\alpha_{em}^{-1}(M_Z) \simeq 128$ and $\sin^2\theta_W(M_Z) \simeq 0.23$, and the SM one-loop RGE. We then allow the Z' coupling at the unification scale $\alpha_U = g_U^2/(4\pi) = g_{Z'}^2(M_U)/(4\pi)$, to vary within the generous bounds

$$\frac{1}{100} < \alpha_U < \frac{1}{20}\,. \tag{2.14}$$

Taking into account that the SM RGE would predict $\alpha_U \sim 1/45$, our upper and lower bounds leave a margin of more than a factor of two to account for threshold corrections, new particles at the TeV scale and other model-dependent effects. Correspondingly, we determine the GUT-favored region of the $(\widetilde{g}_Y, \widetilde{g}_{\mathrm{BL}})$ plane by making use of the one-loop RGE of eqs. (2.11)–(2.13): the result is presented as the colored band in figure 1. The same figure also shows some dots that represent either some popular GUT-inspired benchmark models considered in experimental analyses (the three empty dots and the corresponding dashed lines) or specific SUSY-GUT models with an extra U(1) (the three pairs of full dots). In particular, and in counter-clockwise order: the three dashed lines correspond to the three different models of eq. (2.8), when $g_{Z'}$ is left free to vary; the three empty dots correspond to the GUT-inspired normalization $g_{Z'} = \sqrt{5/3}\,g'(M_Z)$. Instead the SUSY-GUT models are derived properly, using the RGEs: they assume that the GUT group, say SO(10), is broken at M_U into the SM gauge group times an additional U(1) factor, with charges fixed as in eq. (2.8) at the GUT scale. For each of the three models (which correspond, in counter-clockwise order, to those in eq. (2.8)) we draw two black points, corresponding to the RGE evolutions of case (iii) (outer points) and case (iv) (inner points). In both

JHEP11(2009)068

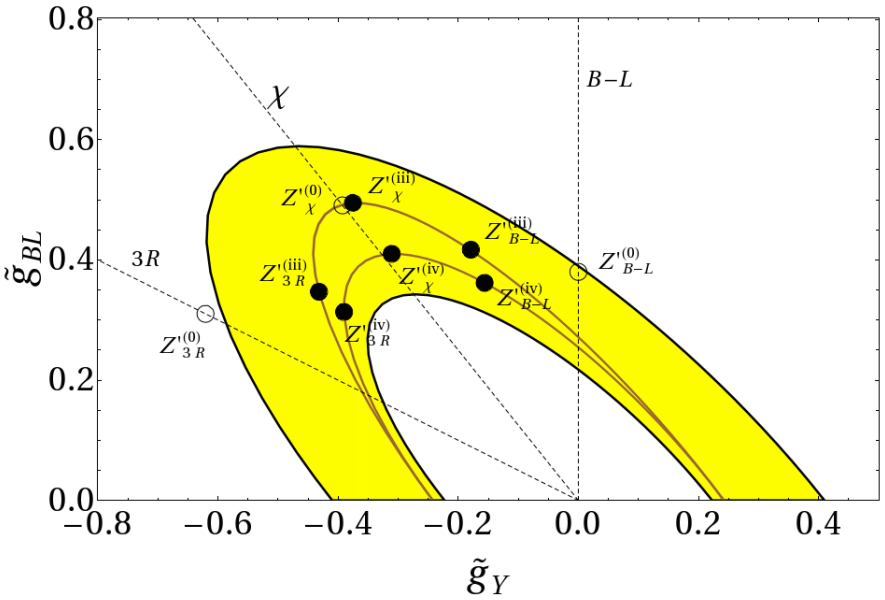

Figure 1. GUT-favored region and some representative models in the $(\widetilde{g}_Y, \widetilde{g}_{\rm BL})$ plane, see the text for details.

cases we get $M_U \sim 2 \times 10^{16}\,\text{GeV}$ and $\alpha_U \sim 1/24$, within the bounds of eq. (2.14). We do not consider non-supersymmetric GUTs among our examples, because they would require the introduction of rather ad hoc exotic fields at intermediate mass scales to match the measured gauge coupling constants at the weak scale. Notice that the introduction of the extra chiral superfields ϕ_1 and ϕ_2 makes the coupling constants g_Y and $g_{\rm BL}$ more 'infrared free' but does not change α_U, thus the values of g_Y and $g_{\rm BL}$ at the weak scale are smaller.

An important point to notice is that, even if we start form a 'pure $B-L$' or 'pure T_{3R}' model at M_U, the mixing effects in the RGE generate, through the resummed large logarithms, sizable corrections to the effective weak-scale couplings, as can be seen from the displacement of the black dots $Z'^{(iii)/(iv)}_{3R/(B-L)}$ from the corresponding dashed lines in figure 1. *With enough running, a specific Z' at the unification scale can turn into a completely different one at the weak scale!* Such effects make clear the advantage of considering the full $(\widetilde{g}_Y, \widetilde{g}_{\rm BL})$ plane to parameterize Z' searches. Notice finally that the direction in the $(\widetilde{g}_Y, \widetilde{g}_{\rm BL})$ plane corresponding to the χ model is quite stable under RGE, because running effects are caused by the MSSM Higgs superfields only. The RGE seem to exhibit an infrared *attractor* towards the region of parameter space with $\widetilde{g}_Y \sim -\widetilde{g}_{\rm BL}$: this fact will become even more interesting after compiling the experimental bounds.

3 Present bounds

3.1 Electroweak precision tests

The use of electroweak precision tests to put bounds on the Z' parameters has a long history. Pre-LEP bounds [14] became much more stringent [15] after LEP1 data at the Z peak, which strongly constrain the mixing angle θ'. However, also higher-energy LEP2 data and

JHEP11(2009)068

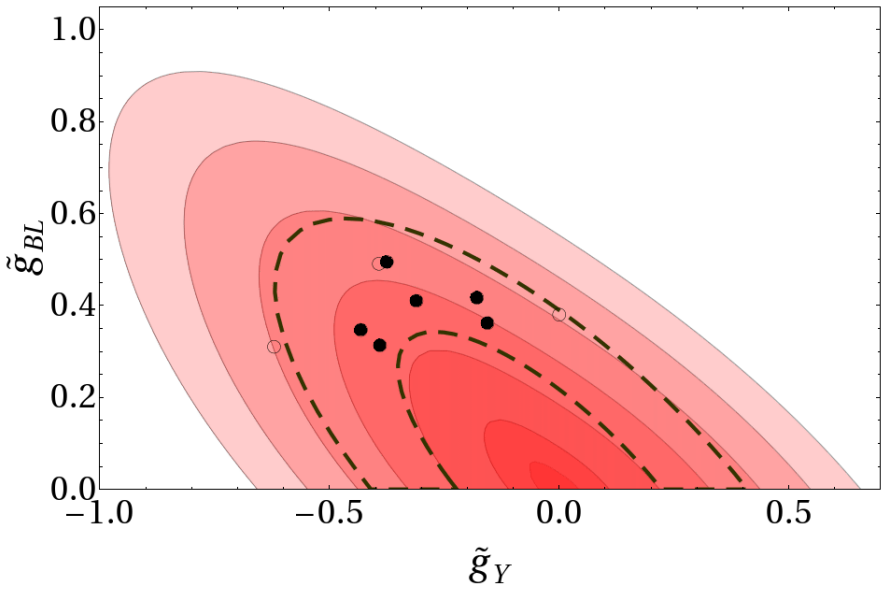

Figure 2. The regions of the $(\widetilde{g}_Y, \widetilde{g}_{\rm BL})$ plane allowed by EWPT, at 95% CL, for $M_{Z'} = 200$, 500, 1000, 1500, 2000, 2500, 3000 GeV (from inner to outer). The GUT-favored region is between the dashed lines.

APV play a very important and complementary rôle in constraining the Z' mass for given couplings, as emphasized for example in [3, 8–11]. In [3] it was shown that the bounds from EWPT can be conveniently rewritten into bounds for the nine EW pseudo-observables ($\hat{S}$, $\hat{T}$, $\hat{U}$, V, W, X, Y, $\delta\epsilon_q$, δC_q). For the case of extra Z' models, these pseudo-observables have simple expressions in terms of the Z' couplings and mass. Once such bounds are rewritten in terms of our parameters ($M_{Z'}$, $\widetilde{g}_Y$, $\widetilde{g}_{\rm BL}$), for each Z' mass we can extract the corresponding 95% CL exclusion regions in the $(\widetilde{g}_Y, \widetilde{g}_{\rm BL})$ plane, as shown in figure 2. The region allowed by EWPT is the red one enclosed by each contour. Dashed lines and empty (full) dots remind us of the GUT-favored region and of the GUT-inspired (-derived) benchmark models. We remind the reader that EWPT only constrain the ratio $g_{Z'}/M_{Z'}$: this explains why the size of the red regions in figure 2 grows linearly with the Z' mass.

It is worth noticing that a recent theoretical re-analysis [4] of the most precise measurements on APV [16] was not included in the fit of ref. [3]. As will be discussed later, the new bounds from APV are significantly stronger than before, but not strong enough yet to compete with the result of the global fit.

It is usually thought that pure $B - L$ models are less constrained by EWPT because of the absence of $Z - Z'$ mixing. Notice however that the region with $\widetilde{g}_Y = 0$ is not particularly favored, actually the region of parameter space least constrained by EWPT is that with $\widetilde{g}_Y \simeq -\widetilde{g}_{\rm BL}$. This feature can be understood by looking at the last row of table 1, which shows that the Z' is less coupled to matter fields, thus less constrained by LEP2 bounds (and by Tevatron bounds as well, as we will see in the next section), roughly when $\widetilde{g}_Y \simeq -\widetilde{g}_{\rm BL}$.

JHEP11(2009)068

	$Z'^{(0)}_{B-L}$	$Z'^{(\mathrm{iii})}_{B-L}$	$Z'^{(\mathrm{iv})}_{B-L}$	$Z'^{(0)}_{\chi}$	$Z'^{(\mathrm{iii})}_{\chi}$	$Z'^{(\mathrm{iv})}_{\chi}$	$Z'^{(0)}_{3R}$	$Z'^{(\mathrm{iii})}_{3R}$	$Z'^{(\mathrm{iv})}_{3R}$
$M_{Z'}$ (TeV)	2.36	1.94	1.68	1.85	1.89	1.57	2.18	1.47	1.33

Table 3. 95% CL bounds on the Z' masses from EWPT, corresponding to the specific models represented by the nine points in figure 1. The $Z'^{(0)}$ models are those represented by empty points, while $Z'^{(\mathrm{iii})}$ ($Z'^{(\mathrm{iv})}$) corresponds to the three external (internal) black points; see the text for details on the choice of the effective couplings.

Notice also the correlation between the orientation of the GUT-favored region of figure 1 (between the dashed contours in figure 2) and the EWPT-allowed regions of figure 2. For all values of the couplings in the GUT-favored region, and in particular for the SUSY-GUT models represented by the full dots, the lower bound on $M_{Z'}$ is above 1 TeV. It is typically above $1.5 \div 2$ TeV for the GUT-inspired benchmark models often considered in the experimental literature. For comparison, we report in table 3 the bounds on the Z' masses for the particular choices of the couplings corresponding to the GUT-inspired and the SUSY-GUT benchmark points[4] of figure 1.

Finally, we comment on the Higgs mass dependence of the bounds above. Since the SM Higgs mass is unknown, we may worry about the stability of our fits to EWPT with respect to varying the Higgs mass. Notice, however, that the dependence of the EWPT on the Higgs mass is only logarithmic and, although Z' bosons may help weakening the EWPT bounds on the Higgs mass [17], in our minimal models the preferred value for the Higgs mass is still below the LEP bound. Varying the Higgs mass within the 95% CL limit from EWPT (which corresponds to $m_h \sim 200$ GeV) produces only a tiny shift in the regions plotted in figure 2. To be definite, we chose $m_h = 120$ GeV as a representative value.

3.2 Tevatron direct searches

Other important bounds on Z' parameters come from direct searches at hadron colliders, presently dominated by the Tevatron experiments CDF and D0. In these experiments, Z' bosons of sufficiently low mass can be produced on-shell and decay in the process $q\bar{q} \to Z' \to \ell^+\ell^-$, ($\ell = e, \mu$). These two are very clean channels to look for: a peak in the invariant mass distribution of e^+e^- or $\mu^+\mu^-$ pairs, with a width controlled by the experimental resolution when the intrinsic Z' width is sufficiently small. The irreducible background is dominated by SM Drell-Yan (DY) $\ell^+\ell^-$ production, which is well understood and whose control is only limited by PDF uncertainties. Other irreducible backgrounds are small and the reducible ones can be easily eliminated by generous cuts. Different decay channels into SM final states have been also experimentally investigated [18], for example $\tau^+\tau^-, jet\ jet, W^+W^-$, but for the minimal models considered here they are not competitive for exclusion or discovery: at best, they could play a rôle in the determination of the Z' couplings after a future discovery.

[4]The alert reader will notice that the bounds in table 3 are numerically stronger than those from figure 2: this is simply because the figure refers to a 2-parameter fit ($\widetilde{g}_Y, \widetilde{g}_{\mathrm{BL}}$), whilst the table refers to specific models, thus to a 1-parameter (M'_Z) fit.

JHEP11(2009)068

The procedure used to extract bounds from such processes has been extensively discussed in the literature (see for example [9, 19]). For a weakly coupled Z', it consists in calculating the Z' production cross-section multiplied by the branching ratio into two charged leptons $\sigma(p\bar{p} \to Z'X) \times \mathrm{BR}(Z' \to \ell^+\ell^-)$ (in our case a function of the three Z' parameters $M_{Z'}$, g_Y, g_{BL}), and comparing it with the limits established by the experiments.

On the theory side, we performed the calculation at NLO in QCD (and LO for the EW part), using the NLO MSTW08 PDF sets [20]. In the calculation of the total width $\Gamma_{Z'}$ we included the following channels: $Z' \to f\bar{f}$, W^+W^-, and Zh, where h is the SM Higgs boson and f are the SM fermions of table 1, with the exception of the right-handed neutrinos, which we took to be heavier than $M_{Z'}/2$. The presence of the two last decay channels is due to $Z - Z'$ mixing and is usually neglected, however for large Z' masses there is an enhancement that cancels the suppression due to the mixing [21, 22]. The ratio $\Gamma_{Z'}/M_{Z'}$ is pretty constant over the whole range of masses of interest, and is around 2% for GUT-favored Z' couplings, and of course smaller for more weakly coupled Z'.

Notice that in the presence of extra matter fields charged under the extra U(1) (light right-handed neutrinos, more light Higgses, supersymmetric partners, etc.), $\Gamma_{Z'}$ would be larger, with a consequent suppression in the branching ratio to charged leptons. In this case the bounds from hadron colliders (and their ability for discovery) would be weaker (unlike those from EWPT, which are quite insensitive to these extensions of the model).

For the Tevatron experimental limit we used the most recent available results from CDF (on $Z' \to e^+e^-$ [5] and $Z' \to \mu^+\mu^-$ [6]) and D0 (on $Z' \to e^+e^-$ [7]). They directly provide the 95% CL bounds on the product $\sigma(p\bar{p} \to Z'\,X) \times BR(Z' \to \ell^+\ell^-)$ based on 2.5, 2.3, 3.6 fb^{-1} of data with $27 \div 38\%$, $13 \div 40\%$, $17 \div 22\%$ total acceptances respectively, with the acceptances growing from smaller to larger values of $M_{Z'}$. Notice that, although D0 data refer to a higher integrated luminosity, the acceptance is smaller, making its bounds a little weaker than those from CDF.

Since not enough information is available to us to properly combine the three sets of data, for each Z' mass we took the strongest bound among the three sets. A combined analysis would be highly welcome as it would probably give stronger bounds.

When compared with the computed cross-section, the experimental limits produce, for each value of $M_{Z'}$, a 95% CL exclusion region in the $(\widetilde{g}_Y, \widetilde{g}_{\mathrm{BL}})$ plane, in analogy with the EWPT case. The results are summarized in figure 3, which shows the 95% CL allowed regions for different M'_Z. Notice that the region favored by GUT models starts becoming accessible for $M'_Z \gtrsim 700\,\mathrm{GeV}$. For masses larger than $\sim 1.2\,\mathrm{TeV}$ the allowed region fills the whole plot, and the available data are no longer able to give useful constraints. Indeed, unlike the EWPT case, the allowed regions in figure 3 grow faster than linearly with $M_{Z'}$, because of the stronger suppression from the x-dependence of the PDF at higher energies.

3.3 Comparison among different bounds

We may wonder whether it makes sense to compare direct and indirect experimental bounds from different experiments, or better whether it is possible to build models that can evade indirect bounds but still be accessible to direct searches. Notice however that indirect LEP searches, low-energy APV experiments, direct and indirect searches at hadron colliders

JHEP11(2009)068

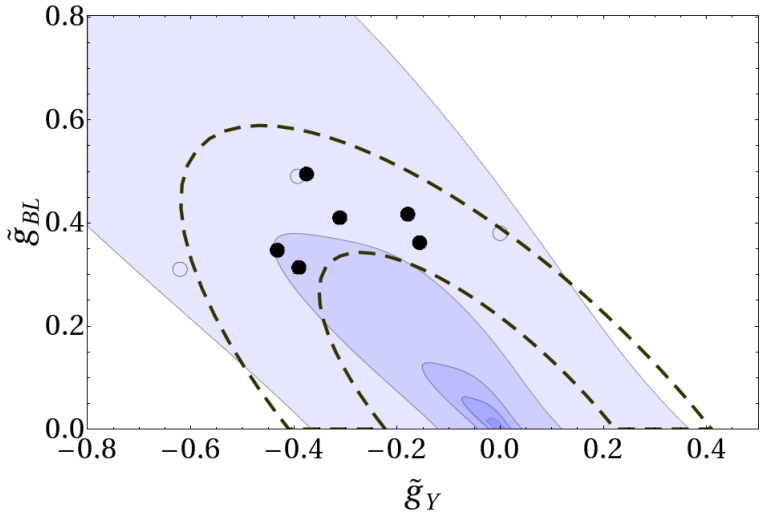

Figure 3. The regions on the $(\widetilde{g}_Y, \widetilde{g}_{\rm BL})$ plane allowed by Tevatron direct searches at 95% CL for $M_{Z'} = 200, 400, 600, 800, 1000\,\text{GeV}$ (from inner to outer). The GUT-favored region is between the dashed lines.

are all basically controlled by tree-level Feynman diagrams built from two basic types of elementary vertices, coupling the Z' to charged leptons and quarks, respectively:

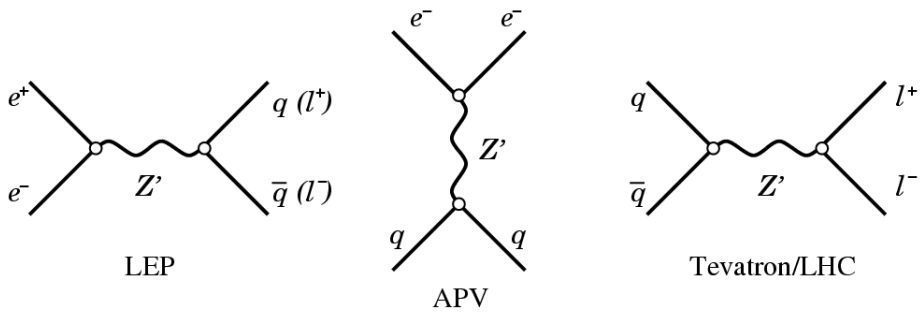

Of course, LEP and APV probe off-shell Z' exchange, whereas the Tevatron and the LHC are sensitive to on-shell Z' production and decay. But the parameters involved in the relevant Feynman diagrams are the same, and it is not easy at all to invent new physics capable of evading indirect bounds from EWPT but still producing a signal in the direct searches. For this reason, the bounds from EWPT should not be neglected when analyzing the discovery reach of direct searches. On the other hand, if the branching ratio to leptons is suppressed by the presence of extra charged matter, then it may happen that indirect searches become even more powerful than the direct ones.

The first thing we notice by comparing the plots in figures 2 and 3 is that both EWPT and Tevatron bounds probe similar regions of the $(\widetilde{g}_Y, \widetilde{g}_{\rm BL})$ plane. In particular, they are both less stringent in the region[5] with $\widetilde{g}_Y \sim -\widetilde{g}_{\rm BL}$, and more stringent in the orthogonal

[5]Remarkably this region seems also to be an attractor of the solutions to the RGE, as commented in the previous section.

JHEP11(2009)068

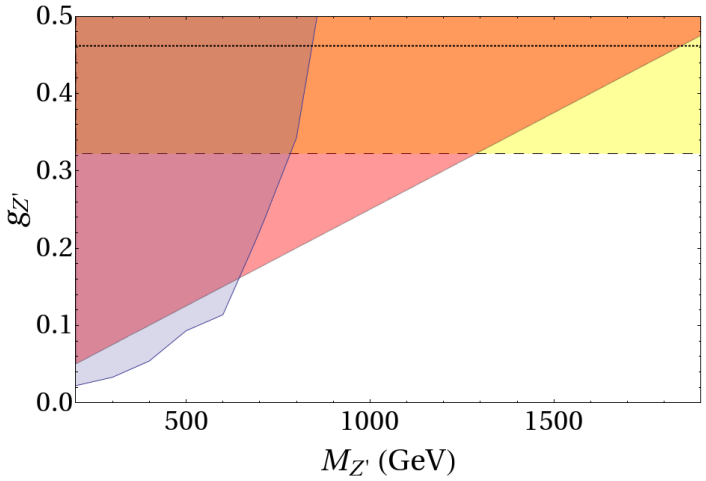

Figure 4. The region of the $(M_{Z'}, g_{Z'})$ plane excluded at 95% CL by EWPT (red) and Tevatron (blue), for the Z_χ model defined in eq. (2.8). The horizontal strip (yellow) recalls the GUT-preferred region and the dotted line the value $g_{Z'} = \sqrt{5/3}\, g'(M_Z)$ corresponding to the $Z'^{(0)}_\chi$ model.

direction (although the actual shape of the exclusion region from the Tevatron is slightly different from that of EWPT). As explained in the previous section, this correlation in the couplings is due to the fact that in the region $\widetilde{g}_Y \sim -\widetilde{g}_{\rm BL}$ there is a partial cancellation in the Z'-charges of the SM fermions (see table 1). Interestingly, also the region preferred by GUT models has the same shape as those allowed by the experimental bounds: this makes the bounds on $M_{Z'}$ at fixed coupling only weakly dependent on the specific nature of the Z'.

Another important difference between the bounds from the Tevatron and from EWPT is that, as already noticed in some previous analyses [3, 8–10], the former give stronger constraints at smaller $M_{Z'}$ but weaker at larger $M_{Z'}$. Indeed, the possibility to produce on-shell Z'-bosons rewards hadron colliders in the mass region that is easily accessible to them. On the other hand, their power rapidly falls off at higher masses because of the PDF dumping at high x. Already for $M_{Z'}$ around 800 GeV, the EWPT bounds start becoming more powerful than the Tevatron limits, independently of the Z' couplings. In particular, all the models with GUT-favored couplings are bound much more strongly by EWPT than by direct searches, at least with the current data.

The competition between the Tevatron and EWPT is more manifest if we plot the bounds as functions of $M_{Z'}$ for a representative model. Figure 4 illustrates the range of Z' masses where the Tevatron gives stronger or weaker constraints compared to EWPT, for a particular direction in the $(\widetilde{g}_Y, \widetilde{g}_{\rm BL})$ plane corresponding to the so-called Z_χ models (the central dashed line in figure 1). Notice that for GUT-favored couplings EWPT give much stronger bounds than the Tevatron. Similar figures were previously shown in refs. [8, 10].

In figure 5, as an illustration, we combine the bounds from EWPT, Tevatron direct searches and the new APV analysis of [4], for the two representative values $M_{Z'} = 400$ and 800 GeV. In the first case the bounds from Tevatron are the strongest for all models, while the APV bounds are the weakest. In the second case we see that EWPT start becoming

JHEP11(2009)068

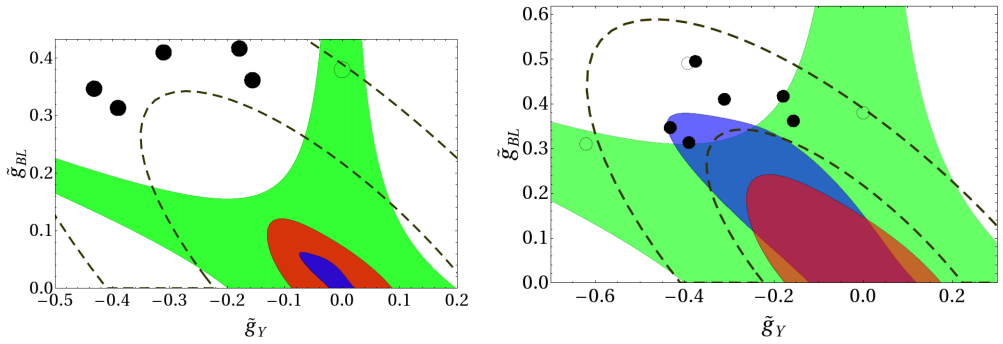

Figure 5. The region of the $(\widetilde{g}_Y, \widetilde{g}_{\rm BL})$ plane allowed by EWPT (red), Tevatron (blue), and APV (green), for $M_{Z'} = 400$ (left) and 800 GeV (right).

stronger than those from the Tevatron in almost all parameter space: for example, Tevatron would still allow an 800 GeV Z'_{3R} with GUT-favored coupling, while EWPT would basically rule out all GUT-like Z' with this mass. APV is always weaker than EWPT but starts becoming stronger than the Tevatron in the region where the latter starts performing worse, i.e. the GUT-preferred region. Notice also that APV experiments are not sensitive to certain types of Z', such as pure $B - L$ that has purely vectorial couplings to fermions. However, as discussed in section 2.2, and evident in figure 5, RGE effects can easily move the Z' couplings away from the safe region, making such Z' models, which would be otherwise safe with respect to APV bounds, also subject to constraints.

The CDF e^+e^- excess. Recently the CDF collaboration [5] observed a small excess of e^+e^- events around 240 GeV, amounting to a $2.5\,\sigma$ fluctuation from the SM background. However, CDF did not see any anomaly in the dimuon spectrum [6]. D0 data [7] at the moment do not seem to confirm nor exclude such excess, also because of the smaller acceptance mentioned before. Although our minimal models would not be able to explain such effect, because of the mismatch between electron and muon spectra, we may still ask whether existing bounds from EWPT may rule out an explanation of the excess in terms of some more general Z' bosons that couple non-universally to leptons, such as those discussed in [23]. Notice from figure 4 that at 240 GeV Tevatron is indeed more sensitive than EWPT to neutral resonances, provided that they have a small coupling, of order $g_{Z'} \sim 0.04$. It turns out that such small coupling would be enough to explain the Tevatron excess without contradicting EWPT.[6] We have not checked whether such scenario is compatible with other flavor non-universal low-energy constraints. More data are anyway required to confirm the presence of a true excess and assess its possible non-standard origin. Notice instead that an analogous signal at energies higher than ∼700 GeV would not be compatible with EWPT, at least within the class of models considered here.

[6]Notice that the same statement can be true also for Z' models very different from those studied in this work [24].

JHEP11(2009)068

4 Early LHC prospects

The questions we want to address in this section are the following. At what combined values of center-of-mass energy and integrated luminosity may we expect the LHC to start having a chance of discovering a Z' (at least of the kind discussed in this work), taking into account all the experimental bounds discussed in the previous sections? What region of parameter space that has not been already ruled out could be accessible for different luminosities and energies in the first LHC runs? Considering the fact that Z' signals are among the cleanest and easiest ones in the search of new physics, our analysis may also be used as a benchmark point when discussing the integrated luminosities that are worth collecting at each energy to actually probe new physics.

At the moment, the program for the first year of LHC running [12] consists in a very first run at low energy ($\sqrt{s} = 7\,\text{TeV}$) and low luminosity ($< 100\ \text{pb}^{-1}$), followed by an upgrade in energy ($\sqrt{s} \leq 10\,\text{TeV}$), with a collected luminosity up to $200 \div 300\ \text{pb}^{-1}$.

At such low[7] energies and luminosities, the constraints from Tevatron direct searches and EWPT play a crucial rôle in identifying the unexcluded region of parameter space that can be probed and the time scale required to have access to it.

Being the LHC a hadron collider, the region of parameter space accessible to it will be similar in shape to the corresponding one at the Tevatron. For relatively light Z' ($M_{Z'} < 800\,\text{GeV}$), since the strongest constraints come from Tevatron direct searches, we expect the LHC to turn into a discovery machine as soon as it becomes sensitive to regions of parameters not yet excluded by the Tevatron. However, while the higher energy is clearly a big advantage for intermediate Z' masses of several hundreds GeV, for lighter masses the low luminosity may be a crucial limiting factor in the early LHC phase. On the other hand, for heavier Z' masses, such as those relevant for GUT models, generically EWPT outperform the Tevatron, and the LHC must wait for higher energies and luminosities to become sensitive.

To turn these considerations into more quantitative statements, we perform a basic analysis along the lines of the one described before for extracting the Tevatron bounds. In the present case we consider the range $\sqrt{s} = 7 \div 10\,\text{TeV}$ for the pp center-of-mass energy, luminosities in the range $50\ \text{pb}^{-1} \div 1\,\text{fb}^{-1}$, and calculate the product $\sigma(pp \to Z'X) \times BR(Z' \to \ell^+\ell^-)$ for $M_{Z'} = 200 \div 3000\,\text{GeV}$, at the same order in perturbation theory as in the Tevatron case. At the same level of precision, we also compute the SM Drell-Yan (DY) differential cross-section, which constitutes the main source of background.

To gain some approximate understanding of the acceptances for signal and background at different values of the invariant mass $M_{\ell^+\ell^-}$ of the $\ell^+\ell^-$ pair, and of the possible model-dependence of the former, we performed a simple study whose results are illustrated in figure 6. For $\sqrt{s} = 10\,\text{TeV}$, we plot the purely geometrical acceptance for signal (solid lines) and SM-DY background (dashed lines), imposing the cut $|\eta| < 2.5$. The colored bands show how much the acceptance varies if the cut is varied from $|\eta| < 2.1$ to $|\eta| < 3.0$. The quantity on the horizontal axis, $[\text{ArcTan}\,(g_Y/g_{\text{BL}})]/\pi$, scans over the different minimal models. The upper blue lines are for $M_{\ell^+\ell^-} = 1\,\text{TeV}$, the lower red lines are for $M_{\ell^+\ell^-} = 200\,\text{GeV}$:

[7] Of course, with respect to the LHC design parameters.

JHEP11(2009)068

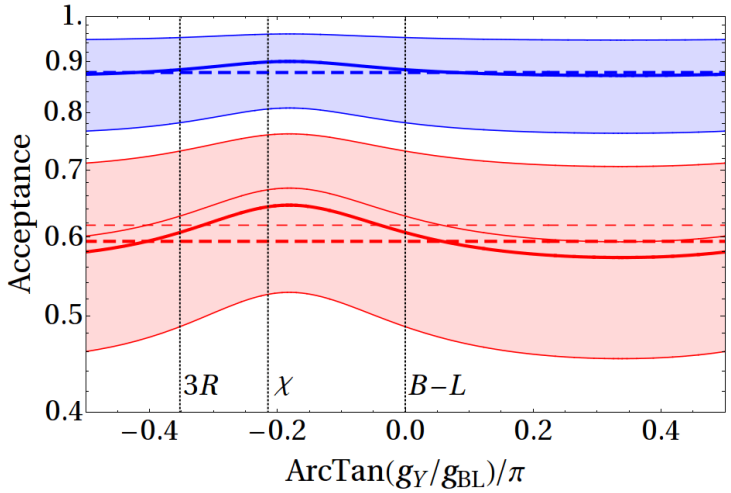

Figure 6. The geometrical acceptance for signal (solid lines) and SM-DY background (dashed lines), as a function of a parameter that scans over the minimal models, and for two representative values of $M_{\ell^+\ell^-}$: 200 GeV (red, lower) and 1 TeV (blue, upper). The different lines refer to the cut $|\eta| < 2.5$ and $p_{T\ell} > 20\,\text{GeV}$ (thin) or $p_{T\ell} > 80\,\text{GeV}$ (thick). The colored bands show how much the acceptance varies by changing the rapidity-cut from $|\eta| < 2.1$ to $|\eta| < 3.0$.

as expected, the acceptance for both signal and background is similar, grows with the invariant mass of the lepton-antilepton pair, and is close to 90% for $M_{\ell^+\ell^-}$ of order 1 TeV or larger. We also looked at how the acceptance depends on the cut on the lepton transverse momenta $p_{T\ell}$: the thin lines correspond to $p_{T\ell} > 20\,\text{GeV}$, the thick ones to $p_{T\ell} > 80\,\text{GeV}$. We can see from figure 6 that this cut is essentially included in the cut on η for high mass values, whereas it has a small but non-negligible effect on the acceptance for low mass values. Finally, the model-dependence also decreases when moving from lower to higher masses, and is never larger than 10% even for $M_{Z'} \sim 200\,\text{GeV}$. In view of these results, and for the purposes of the present exploratory study, we then assumed an acceptance depending only on the invariant mass, as done for example in ref. [25]. Our computed values of the acceptance are compatible with those of ref. [25], thus we adopt their figure 2 for the rest of our LHC study. More refined studies, however, should take into account also the model-dependence of the acceptance, which may not be negligible for Z' searches at relatively small masses.

To estimate the 5σ discovery reach of the early phase of the LHC [25–27], we compared the events due to a generic Z' signal to the events from the SM-DY background in a 3% interval around the relevant values of the dilepton invariant mass.[8] We then required the signal events to be at least a 5σ fluctuation over the expected background, and in any case more than 3. This rough statistical analysis is enough to get an approximate answer to the questions we want to address. We leave a more careful analysis to the experimental collaborations ATLAS and CMS, which have control on all the information needed to

[8]This should be compatible with the expected energy resolution, even in this early phase, and with the fact that, for GUT-favored values of the coupling constants, $\Gamma_{Z'}/M_{Z'} \sim 2\%$.

JHEP11(2009)068

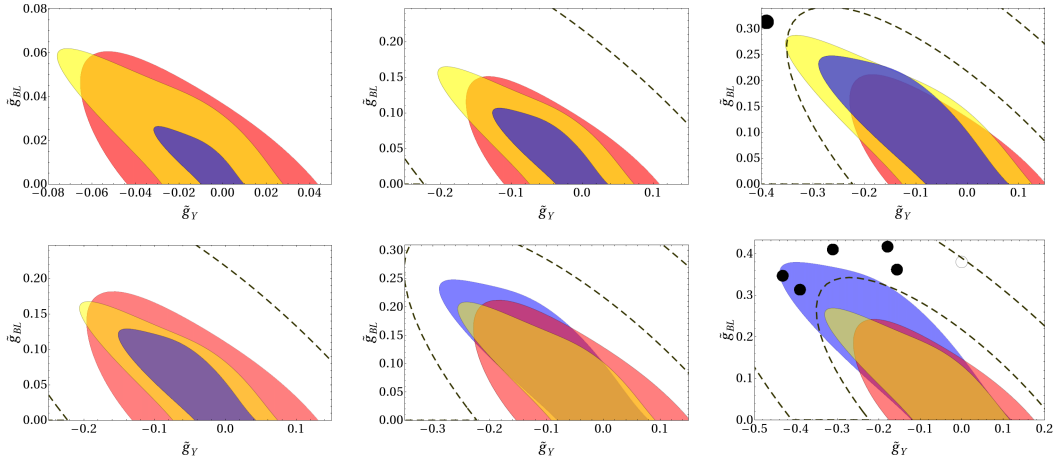

Figure 7. The LHC 5σ discovery potential in the $(\widetilde{g}_Y, \widetilde{g}_{\rm BL})$ plane for $\sqrt{s} = 7\,\text{TeV}$. The red and blue regions are those allowed by EWPT and Tevatron bounds respectively; the yellow region is the one not within 5σ discovery reach at the LHC. Thus the region accessible by the LHC is the one formed by points that are both in the red and blue regions but not in the yellow one. Plots in the first row refer to 50 pb^{-1} of data and $M_{Z'} = 200,\ 500,\ 700\,\text{GeV}$ respectively; plots in the second row are for 100 pb^{-1} of data and $M_{Z'} = 600,\ 700,\ 800\,\text{GeV}$ respectively.

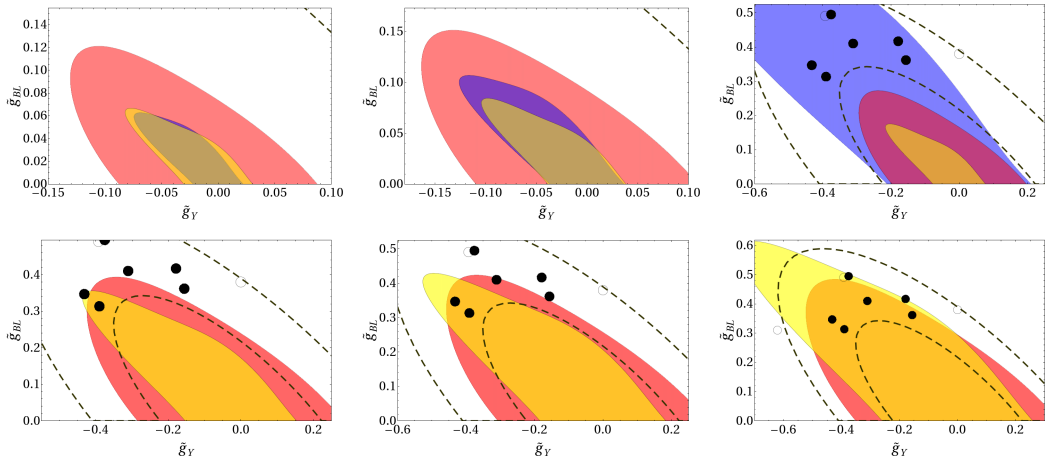

Figure 8. The LHC 5σ discovery potential in the $(\widetilde{g}_Y, \widetilde{g}_{\rm BL})$ plane for $\sqrt{s} = 10\,\text{TeV}$, 200 pb^{-1} of data and $M_{Z'} = 400,\ 500,\ 900,\ 1300,\ 1400,\ 1600\,\text{GeV}$. The meaning of the colored regions is as in figure 7. In the last three plots the Tevatron bounds are not shown because they are too weak to give useful constraints.

perform it in an accurate and reliable way. A more refined analysis would also be needed for a possible Z' diagnostics after discovery, as studied for example in [28].

We present sample plots in figures 7 and 8. Besides the regions allowed by EWPT and Tevatron data (red and blue) we plotted, for each representative value of the Z' mass, and of the LHC energy and integrated luminosity, the region not accessible to the LHC (in yellow) for a 5σ discovery as defined above. We see that $\sqrt{s} = 7\,\text{TeV}$ and 50 pb^{-1} are not enough to discover any Z' in the whole parameter space considered; in particular at low masses the low luminosity makes the LHC underperform with respect to the Tevatron,

JHEP11(2009)068

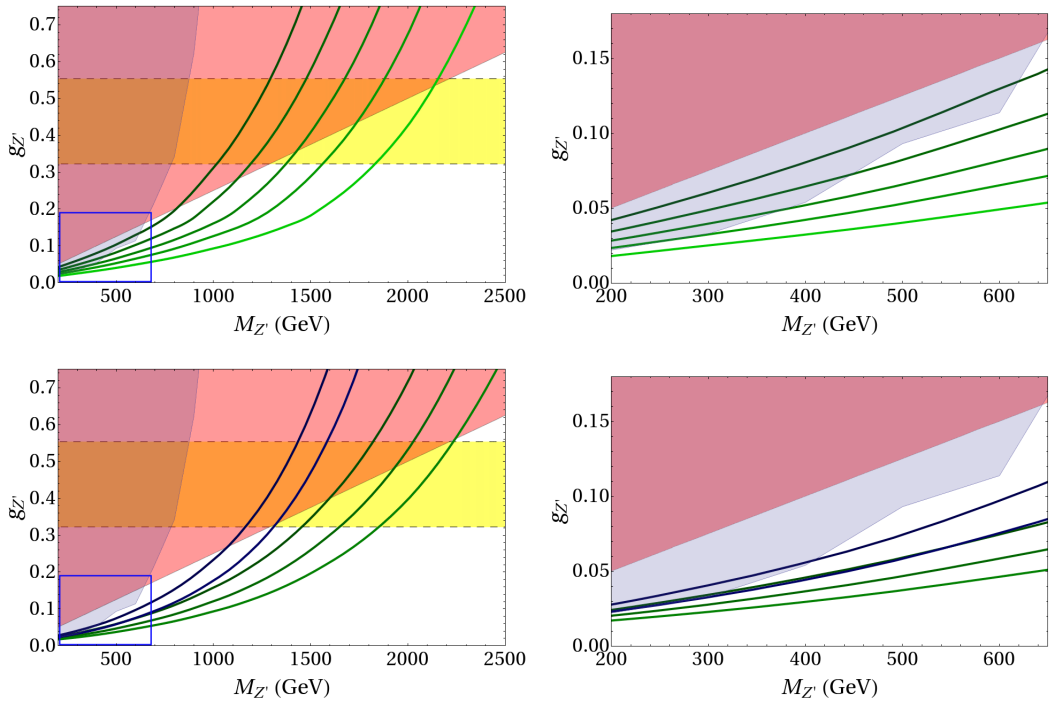

Figure 9. *First row.* The region of the $(M_{Z'}, g_{Z'})$ plane amenable to a '5σ' discovery at the LHC, for the Z_χ model, $\sqrt{s} = 10\,\text{TeV}$ and some representative values of the integrated luminosity; from left to right: 50, 100, 200, 400 and 1000 pb^{-1}. The red and blue region and the yellow band are the same as in figure 4. The second box is a zoom on the low-mass, low-coupling region. *Second row.* 95% CL exclusion contours from the LHC after 50 and 100 pb^{-1} at $\sqrt{s} = 7\,\text{TeV}$ (blue curves) and after 50, 100 and 200 pb^{-1} at $\sqrt{s} = 10\,\text{TeV}$ (green curves).

while at masses where the LHC starts having a kinematical advantage over the Tevatron, both cannot compete anymore with EWPT. With 100 pb^{-1} of data at the same energy, a first non-excluded region of parameters becomes accessible to discovery, though it is very narrow ($M_{Z'} \sim 700 \pm 100\,\text{GeV}$ and $\widetilde{g}_{\text{BL}} \sim 0.15 \div 0.20$, $\widetilde{g}_Y \sim -0.2 \div 0$).

Things start improving as the LHC steps up in energy and luminosity. The situation with $\sqrt{s} = 10\,\text{TeV}$ and 200 pb^{-1} of integrated luminosity is represented in figure 8. The region of Z' masses below 400 GeV will not be accessible yet, this because the higher luminosity collected at the Tevatron is more important in such energy region. The first accessible zone in parameter space starts showing up for $M_{Z'} \sim 400 \div 1100\,\text{GeV}$, for models with couplings smaller than those preferred by GUTs, and for $M_{Z'} \sim 1200 \div 1500\,\text{GeV}$ for GUT-like couplings. For heavier Z' no region is left to the LHC that is not already ruled out by EWPT. As evident from the plots, for each of the accessible Z' masses, only a small portion of the $(\widetilde{g}_Y, \widetilde{g}_{\text{BL}})$ plane will be tested. Our plots refer to data collected by a single experiment and for a single dilepton channel, combining the data might help increasing the effective luminosity collected and thus the discovery potential.

Since contour plots may require some patience to be interpreted, we make our results more manifest by plotting, in figure 9, the 5σ LHC discovery potential in the $(M_{Z'}, g_{Z'})$

JHEP11(2009)068

plane for the representative χ model. As in figure 4, the red and blue regions are those presently excluded by EWPT and Tevatron direct searches, respectively, and the yellow band denotes the GUT-favored region. The new curves enclose the region where a 5σ discovery at the LHC is in principle possible, for $\sqrt{s} = 10\,\text{TeV}$ and some representative values of the integrated luminosity: 50, 100, 200, 400 and 1000 pb^{-1}, from left to right. Notice that, in the case under consideration, the first mass region to be touched is between 600 and 800 GeV, with the region enlarging towards higher mass values with increasing luminosity. We start entering the GUT-favored region of parameters only for 100 pb^{-1}, and 1 fb^{-1} is enough to reach mass values as high as 2 TeV, with a full coverage of the GUT-favored region of couplings. Notice also that the access to lower mass values is also gradual, and that $1\,\text{fb}^{-1}$ is required to do better than the Tevatron at $M_{Z'} \sim 200\,\text{GeV}$. We have performed a similar analysis for $\sqrt{s} = 7\,\text{TeV}$: in such a case, 400 pb^{-1} give approximately the same sensitivity as 200 pb^{-1} at 10 TeV for $M_{Z'} < 700\,\text{GeV}$, whilst the sensitivity at higher mass values rapidly becomes worse and worse, as expected: there are no doubts that it is worth raising the LHC energy as soon as it can be safely done.

Of course, if no discrepancy from the SM is found in the dilepton spectra, LHC will be able to improve the 95% CL bounds on minimal Z' models already after the first run(s). Indeed, as shown in figure 9, 100 pb^{-1} at $\sqrt{s} = 7\,\text{TeV}$ are already enough to top both Tevatron and EWPT bounds for all Z' masses up to 1.3 TeV, while, after the first year of run, LHC might be able to rule out most of the GUT-preferred region below $\sim 2\,\text{TeV}$.

In summary, our study shows how strong the rôle played by the existing experimental bounds can be in limiting the access to new physics in the early LHC phase. Even for the 'easy' Z' models usually considered, the energy and luminosity required to overcome existing bounds can delay the possibility of discovering new physics by a non-negligible amount. The importance of reaching higher energies and luminosities is clear, as it is the importance of combining data from different detectors and channels already in this early phase.

Our analysis also shows that different regions in parameter space will become available for discovery at different times, depending on the energies and luminosity reached. Hence it would be sensible to switch to general parameterizations such as the one described in the present work, which are not as restrictive as those commonly used at the moment. The latter may focus the attention on the 'wrong' regions of parameter space that are already ruled out by current data, instead of those with the greatest potential to host accessible new physics.

Acknowledgments

We thank H. Burkhardt, R. Contino, S. Forte, L. Ibáñez, M. Pierini, G. Ridolfi, A. Strumia, E. Torassa and A. Uranga for discussions. This work was partially supported by the Fondazione Cariparo Excellence Grant *String-derived supergravities with branes and fluxes and their phenomenological implications.*

JHEP11(2009)068

References

[1] M.C. Chen and B.A. Dobrescu, *Z'-Boson Searches*, in Particle Data Group collaboration, C. Amsler et al., *Review of particle physics*, *Phys. Lett.* **B 667** (2008) 1; P. Langacker, *The Physics of Heavy Z' Gauge Bosons*, arXiv:0801.1345 [SPIRES].

[2] T. Appelquist, B.A. Dobrescu and A.R. Hopper, *Nonexotic neutral gauge bosons*, *Phys. Rev.* **D 68** (2003) 035012 [hep-ph/0212073] [SPIRES].

[3] G. Cacciapaglia, C. Csáki, G. Marandella and A. Strumia, *The minimal set of electroweak precision parameters*, *Phys. Rev.* **D 74** (2006) 033011 [hep-ph/0604111] [SPIRES].

[4] S.G. Porsev, K. Beloy and A. Derevianko, *Precision determination of electroweak coupling from atomic parity violation and implications for particle physics*, *Phys. Rev. Lett.* **102** (2009) 181601 [arXiv:0902.0335] [SPIRES].

[5] CDF collaboration, T. Aaltonen et al., *Search for High-Mass e^+e^- Resonances in $p\bar{p}$ Collisions at $\sqrt{s}$ = 1.96-TeV*, *Phys. Rev. Lett.* **102** (2009) 031801 [arXiv:0810.2059] [SPIRES].

[6] CDF collaboration, T. Aaltonen et al., *A search for high-mass resonances decaying to dimuons at CDF*, *Phys. Rev. Lett.* **102** (2009) 091805 [arXiv:0811.0053] [SPIRES].

[7] D0 collaboration, *Search for high-mass narrow resonances in the di-electron channel at D0*, D0 Note 5923-CONF, July 2009.

[8] R. Barbieri, A. Pomarol, R. Rattazzi and A. Strumia, *Electroweak symmetry breaking after LEP-1 and LEP-2*, *Nucl. Phys.* **B 703** (2004) 127 [hep-ph/0405040] [SPIRES].

[9] M.S. Carena, A. Daleo, B.A. Dobrescu and T.M.P. Tait, *Z' gauge bosons at the Tevatron*, *Phys. Rev.* **D 70** (2004) 093009 [hep-ph/0408098] [SPIRES].

[10] R. Contino, Z', Z_{KK}, Z^* *and all that: Current bounds and theoretical prejudices on heavy neutral vector bosons*, *Nuovo Cim.* **123B** (2008) 511 [arXiv:0804.3195] [SPIRES].

[11] J. Erler, P. Langacker, S. Munir and E.R. Pena, *Improved Constraints on Z' Bosons from Electroweak Precision Data*, *JHEP* **08** (2009) 017 [arXiv:0906.2435] [SPIRES].

[12] H. Burkhardt, *Status of the LHC Machine*, plenary talk at *Lepton-Photon 2009*, Hamburg, Germany, 16-22 August 2009, to appear in the Proceedings; M. Lamont, *LHC Operations 2009/2010*, talk given to the ATLAS Collaboration, 27 August 2009.

[13] B. Holdom, *Two U(1)'s and Epsilon Charge Shifts*, *Phys. Lett.* **B 166** (1986) 196 [SPIRES].

[14] U. Amaldi et al., *A Comprehensive Analysis of Data Pertaining to the Weak Neutral Current and the Intermediate Vector Boson Masses*, *Phys. Rev.* **D 36** (1987) 1385 [SPIRES]; G. Costa, J.R. Ellis, G.L. Fogli, D.V. Nanopoulos and F. Zwirner, *Neutral Currents Within and Beyond the Standard Model*, *Nucl. Phys.* **B 297** (1988) 244 [SPIRES].

[15] G. Altarelli, R. Casalbuoni, D. Dominici, F. Feruglio and R. Gatto, *Testing for heavier vector bosons in e^+e^- at Z peak: a comparative study of different models*, *Nucl. Phys.* **B 342** (1990) 15 [SPIRES]; F. del Aguila, W. Hollik, J.M. Moreno and M. Quirós, *Correlation between $M_{Z'}$ and M_t bounds. 2. All data*, *Nucl. Phys.* **B 372** (1992) 3 [SPIRES]; P. Langacker and M.-x. Luo, *Constraints on additional Z bosons*, *Phys. Rev.* **D 45** (1992) 278 [SPIRES].

JHEP11(2009)068

[16] C.S. Wood et al., *Measurement of parity nonconservation and an anapole moment in cesium*, *Science* **275** (1997) 1759 [SPIRES];
S.C. Bennett and C.E. Wieman, *Measurement of the 6S → 7S transition polarizability in atomic cesium and an improved test of the standard model*, *Phys. Rev. Lett.* **82** (1999) 2484 [hep-ex/9903022] [SPIRES].

[17] A. Ferroglia, A. Lorca and J.J. van der Bij, *The Z′ reconsidered*, *Annalen Phys.* **16** (2007) 563 [hep-ph/0611174] [SPIRES];
M.S. Chanowitz, *A Z′ Boson and the Higgs Boson Mass*, arXiv:0806.0890 [SPIRES].

[18] CDF collaboration, D.E. Acosta et al., *Search for new physics using high mass tau pairs from 1.96 TeV $p\bar{p}$ collisions*, *Phys. Rev. Lett.* **95** (2005) 131801 [hep-ex/0506034] [SPIRES];
CDF collaboration, T. Aaltonen et al., *Search for new particles decaying into dijets in proton- antiproton collisions at $\sqrt{s} = 1.96$ TeV*, *Phys. Rev.* **D 79** (2009) 112002 [arXiv:0812.4036] [SPIRES];
CDF collaboration, *Search for diboson (W^+W^- or $W^\pm Z^0$) resonances in electron, missing E_T and two jets final state*, CDF Note CDF/PUB/EXOTIC/PUBLIC/9730, April 2009.

[19] P. Langacker, R.W. Robinett and J.L. Rosner, *New Heavy Gauge Bosons in p p and $p\bar{p}$ Collisions*, *Phys. Rev.* **D 30** (1984) 1470 [SPIRES];
V.D. Barger, N.G. Deshpande, J.L. Rosner and K. Whisnant, *Production, Decays and Forward Backward Asymmetries of Extra Gauge Bosons In E_6*, *Phys. Rev.* **D 35** (1987) 2893 [SPIRES];
F. del Aguila, M. Quirós and F. Zwirner, *Detecting E_6 Neutral Gauge Bosons Through Lepton Pairs at Hadron Colliders*, *Nucl. Phys.* **B 287** (1987) 419 [SPIRES];
J.R. Ellis, P.J. Franzini and F. Zwirner, *Limits on the mass of a superstring Z′ from the CERN $p\bar{p}$ collider*, *Phys. Lett.* **B 202** (1988) 417 [SPIRES];
J. Kang and P. Langacker, *Z′ discovery limits for supersymmetric E_6 models*, *Phys. Rev.* **D 71** (2005) 035014 [hep-ph/0412190] [SPIRES];
B. Fuks, M. Klasen, F. Ledroit, Q. Li and J. Morel, *Precision predictions for Z′ - production at the CERN LHC: QCD matrix elements, parton showers and joint resummation*, *Nucl. Phys.* **B 797** (2008) 322 [arXiv:0711.0749] [SPIRES].

[20] A.D. Martin, W.J. Stirling, R.S. Thorne and G. Watt, *Parton distributions for the LHC*, *Eur. Phys. J.* **C 63** (2009) 189 [arXiv:0901.0002] [SPIRES].

[21] F. del Aguila, M. Quirós and F. Zwirner, *On the mass and the signature of a new Z*, *Nucl. Phys.* **B 284** (1987) 530 [SPIRES].

[22] S. Nandi, *Higgs boson production at heavy Z resonance*, *Phys. Lett.* **B 181** (1986) 375 [SPIRES];
H. Baer, D. Dicus, M. Drees and X. Tata, *Higgs Boson Signals in Superstring Inspired Models at Hadron Supercolliders*, *Phys. Rev.* **D 36** (1987) 1363 [SPIRES];
V.D. Barger and K. Whisnant, *Heavy Z boson decays to two Bosons in E_6 superstring models*, *Phys. Rev.* **D 36** (1987) 3429 [SPIRES].

[23] M.-C. Chen, A. de Gouvêa and B.A. Dobrescu, *Gauge trimming of neutrino masses*, *Phys. Rev.* **D 75** (2007) 055009 [hep-ph/0612017] [SPIRES].

[24] O. Catà, G. Isidori and J.F. Kamenik, *Drell-Yan production of Heavy Vectors in Higgsless models*, *Nucl. Phys.* **B 822** (2009) 230 [arXiv:0905.0490] [SPIRES].

[25] CMS collaboration, *Search for New High-Mass Resonances Decaying to Muon Pairs in the CMS Experiment*, CMS PAS SBM-07-002.

JHEP11(2009)068

[26] The ATLAS collaboration, G. Aad et al., *Expected Performance of the ATLAS Experiment. Detector, Trigger and Physics*, arXiv:0901.0512 [SPIRES].

[27] CMS collaboration, *Search for high mass resonance production decaying into an electron pair in the CMS experiment*, CMS PAS EXO-08-001; *Search for high mass resonances decaying into an electron pair in CMS at 10 TeV with 100 pb^{-1}*, CMS PAS EXO-09-006.

[28] F. del Aguila, M. Cvetič and P. Langacker, *Determination of Z-prime gauge couplings to quarks and leptons at future hadron colliders*, *Phys. Rev.* **D 48** (1993) 969 [hep-ph/9303299] [SPIRES];
M. Dittmar, A.-S. Nicollerat and A. Djouadi, *Z' studies at the LHC: An update*, *Phys. Lett.* **B 583** (2004) 111 [hep-ph/0307020] [SPIRES];
F. Petriello and S. Quackenbush, *Measuring Z' couplings at the CERN LHC*, *Phys. Rev.* **D 77** (2008) 115004 [arXiv:0801.4389] [SPIRES];
P. Osland, A.A. Pankov, A.V. Tsytrinov and N. Paver, *Spin and model identification of Z' bosons at the LHC*, *Phys. Rev.* **D 79** (2009) 115021 [arXiv:0904.4857] [SPIRES];
Y. Li, F. Petriello and S. Quackenbush, *Reconstructing a Z' Lagrangian using the LHC and low-energy data*, *Phys. Rev.* **D 80** (2009) 055018 [arXiv:0906.4132] [SPIRES].

JHEP11(2009)068